Vulnerability and Resilience of National Power Grids: A Graph-Theoretical Optimization Approach and Empirical Simulation

Jean-Claude Metzger, Saša Parađ, Stefan Ravizza, and Marcus M. Keupp

1 Introduction

Modern societies must rely on a working electrical power distribution system, i.e. a power grid that supplies instantaneously all the required demand. System failure can lead to uncovered power demand, such that infrastructures and public services which rely on electrical power are significantly impaired or even terminated (e.g., public transport, drinking water supply, telecommunications, etc.).

Further, initial failure in a particular area of the power grid can result in a sequence of cascading failures that spreads through both the domestic and the international grid, implying black-outs in whole regions or even countries [12]. This effect is illustrated by actual black-out events from the recent past, e.g. in Italy [15], the north-east USA and Canada [13] and India [18]. These and other power grids have been investigated over the last two decades [7, 11]. The analysis

J.-C. Metzger
hemotune AG, Zurich, Switzerland
e-mail: jean-claude.metzger@hemotune.ch

S. Parađ
Valucor Group AG, Zurich, Switzerland

Valucor (FL) AG, Vaduz, Liechtenstein
e-mail: sascha.parad@valucor.ch

S. Ravizza
IBM Switzerland Ltd., Zurich, Switzerland
e-mail: stefan.ravizza@ch.ibm.com

M. M. Keupp (✉)
Department of Defense Economics, Military Academy at the Swiss Federal Institute of Technology Zurich, Birmensdorf, Switzerland
e-mail: mkeupp@ethz.ch

M. M. Keupp (ed.), *The Security of Critical Infrastructures*, International Series in Operations Research & Management Science 288,
https://doi.org/10.1007/978-3-030-41826-7_6

of power grids as graphs using graph theory is useful and productive (see [10] for a review). Prior research has analyzed topological patterns of nodes, edges and their links [1, 6]. Other studies provide dynamic analyses of potential black-out situations [7, 11]. Further, technical work has focused on the electro-physical properties of a power grid by enriching graphs with impedances [4] and complete AC models [3]. However, the majority of extant work focuses on a worst-case scenario by which the removal of a critical node or edge from the grid results in cascading failure that eventually causes a black-out. By contrast, in this chapter we propose that less-than-worst-case scenarios deserve equal attention. In particular, we focus on scenarios in which the grid can satisfy partially, but not completely, any given demand for power.

Power grids are subject to the fundamental electro-physical restriction that all power demand must be in equilibrium with all power supply at all times. If this condition is not met, the grid frequency will deviate from the ideal target value of $f = 50\,\text{Hz}$. A deviation as small as 2.5 Hz can already result in resonance oscillations and subsequent turbine damage [16].

Hence, a sudden drop of supply will result in a power shortage situation that requires shedding some of the electrical load (demand). By the same token, if a sudden drop in demand occurs, supply must also be reduced immediately. In both cases, uncovered demand (UD) results. The focus of our analysis is to provide a dynamic model of how UD develops as a result of node or edge removal.

We first discuss how a power grid network can be modeled as a graph and how linear programming can be used to simulate UD. Furthermore, quantitative measures are introduced which capture the reduction of grid performance as a function of node or edge removal. Section 3 presents how the vulnerability of a power grid can be analyzed by the systematic modeling of different attack strategies. Section 4 illustrates this analysis with topological and capacity data from the Swiss maximum voltage power grid. Section 5 develops some recommendations for building robust and resilient power networks.

2 Analyzing Power Grids Using Graph Theory

A power grid can be described as a set of elements that supply power (power plants), demand power (industry, individuals) or transform power between voltage levels. Those elements are connected to each other by power transmission lines that transfer power throughout the network. The totality of all elements and transmission lines can be modeled as a directed graph $G = (V, E)$, where V is a set of nodes and E the set of links between those nodes. Each transmission line is modeled by two directed edges that point to either the supplying or the receiving node.

Nodes can either supply to or demand power from the network or do both. Hence, for each node i the *net demand* is calculated as

$$y_i = supply_i - demand_i, \forall i \in N \tag{1}$$

where N is the total number of nodes.

While demand is modeled as a fixed value, the supply values of particular providers, such as pumped storage power stations, can vary between a minimum supply value $supply_i^{min}$ and a maximum supply value $supply_i^{max}$. Hence, the resulting net demand values y_i are bounded for each node i by

$$y_i^{min} \leq y_i \leq y_i^{max} \tag{2}$$

where $y_i^{min} = supply_i^{min} - demand_i$ and $y_i^{max} = supply_i^{max} - demand_i$.

Electricity imports from or to neighboring countries are modeled by the demand and supply of those (foreign) nodes that are adjacent to the focal country's border and connected to its internal power grid. Imported power is treated as supply and has therefore a lower and an upper supply boundary, while exported power is treated as demand and kept at a constant level $demand_i$.

The power flow of each edge is noted by x_{ij} for the edge transferring power from node i to node j and x_{ji} for the edge transferring power in the opposite direction, i.e. from node j to node i. The flows on those edges are also bounded by the physical capacity limit of the transmitting power line:

$$0 \leq x_{ij} \leq x_{ij}^{max} \tag{3}$$

One of the two flows between two nodes will always be zero while the other one defines the direction of the flow. If there is no power flow between two nodes then both edges will have the value zero.

Eventually, for each node i the difference of the outgoing and the incoming flows must equal the *net demand* of this node:

$$\underbrace{\sum_{(j,i)\in E} x_{ji}}_{outgoing\ flow} - \underbrace{\sum_{(i,k)\in E} x_{ik}}_{incoming\ flow} = y_i \quad \forall i \in N \tag{4}$$

Figure 1 shows a small example of a graph with seven nodes and fourteen edges. Node 7 is an auxiliary node that connects nodes 2, 4 and 5 to each other.[1]

2.1 Power Flow Calculation Using Linear Programming

In order to verify if the overall supply of a network can cover all demand by means of the existing transmission lines, the optimization problem specified by Eqs. (5)–(8) has to be solved. It is stated as a linear programming formulation where the overall

[1]While this auxiliary node neither demands nor supplies any power, it is required to reflect the tripartite connection between nodes 2, 4, and 5.

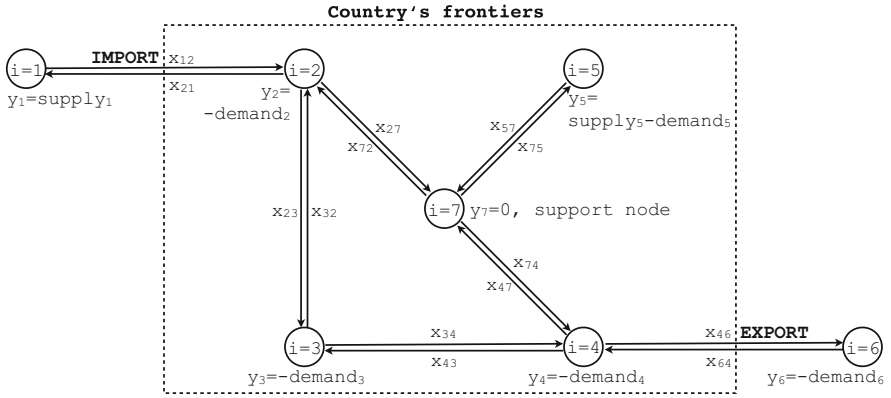

Fig. 1 This small sample network imports power from abroad via node 1 ($x_{12} = supply_1$ and $x_{21} = 0$) and exports power to node 6 ($x_{46} = -demand_6$ and $x_{64} = 0$). Nodes 2, 3 and 4 only demand power while node 5 supplies and demands power

power flow over all transmission lines is minimized (5). Hence, the overall loss from power transmission is minimized.[2] Inequalities (6) and (7) are calculated by placing Eq. (4) into the inequalities of Eq. (2). Equation (8) defines lower and upper bounds on the power flow variable x. It reflects the physical power flow limitations of the network's transmission lines.

Optimization problem (linear programming)

$$min \sum_{(i,j)\in E} x_{ij} \tag{5}$$

$$\underbrace{\sum_{(j,i)\in E} x_{ji}}_{outgoing flow} - \underbrace{\sum_{(i,k)\in E} x_{ik}}_{incoming flow} \leq y_i^{max} \quad \forall i \in N \tag{6}$$

$$-\underbrace{\sum_{(j,i)\in E} x_{ji}}_{outgoing flow} + \underbrace{\sum_{(i,k)\in E} x_{ik}}_{incoming flow} \leq -y_i^{min} \quad \forall i \in N \tag{7}$$

$$x_{ij}^{min} \leq x_{ij} \leq x_{ij}^{max} \quad \forall (i,j) \in E \tag{8}$$

An optimal solution for this LP not only proves that a network exists that can satisfy all demands. It also highlights which edges are transferring more power than others and hence illustrates that edges may differ in terms of their strategic

[2] By this approach, our model reflects engineers' attempts to minimize transmission loss as they operate real power networks.

importance for the network. The absolute power flow on a network's transmission line is calculated over the two edges connecting two nodes by $|x_{ij} - x_{ji}| \; \forall (i, j) \in E$.

2.2 (N-1) Analysis and Resulting Uncovered Demand

The failure of both nodes and edges can result in reduced network performance. An (N-1) analysis can identify the extent to which this is the case by analyzing the consequences of node removal for the remaining network's performance. Analogously, an (E-1) analysis can analyze those consequences when edges are removed. The node removal analysis comprises the following sequence of steps.

Step 1 Remove a node j and identify the edges connecting other nodes to node j. Delete also those connecting edges.

Step 2 Check if the remaining nodes and edges have been split into subgraphs.[3]

Step 3 Conduct for each subgraph the optimization problem as stated in Eqs. (5)–(8).

Step 4 If no solution to the optimization problem could be found, the demand of the subgraph is iteratively reduced by setting demands to zero (starting with the smallest demand within the subgraph) until a solution to the optimization problem is found or the demand of the subgraph cannot be reduced further.

Step 5 The covered demand and power flows of the subgraphs are stored.

Finally, we introduce the following quantitative measures for the analysis of the resulting graph or set of subgraphs.

Uncovered Demand (UD) Uncovered demand (UD) measures the reduced network performance, i.e. the percentage of any demand that cannot be covered after a node j has been removed:

$$UD = 100\% - \frac{100\%}{total\_demand_N} \cdot total\_demand_{(N-1)} \tag{9}$$

with

$$total\_demand_N = \sum_{i \in N} demand_i$$

$$total\_demand_{(N-1)} = \sum_{i \in N \setminus j} demand_i$$

[3] It is possible that the original graph is split into subgraphs upon node removal. For example, in Fig. 1 the removal of node 7 generates a subgraph that comprises only node 5, and another subgraph that comprises all other nodes.

This measure can be applied repeatedly, such that uncovered demand in the case of repeated node removal can also be calculated.

Residual Flow Capacity (RFC) Residual flow capacity (RFC) measures the extent to which any unused capacity is available on any transmission line $(i, j) \in E$:

$$RFC_{ij} = 100\% - \frac{100\%}{x_{ij}^{max}} \cdot (x_{ij}^{max} - x_{ij}) \tag{10}$$

This measure allows us to identify edges that are approaching their physical transmission capacity limit.

3 Vulnerability Analysis of Power Grids

Our analysis focuses on conscious and deliberate attacks against the power grid, whereas the analysis of random damage caused by natural disasters or hardware failure is beyond the scope of this chapter. Deliberate attack patterns target specific elements in the network that are easy to reach, have little resilience, or prove to be critical for network performance. In the following, we propose different operationalizations of such deliberate attack patterns, adopting the viewpoint of the attacker. A power grid can be deliberately attacked by removing single or multiple elements of the network, i.e. nodes, edges, or both.

3.1 Node Removal

Supply Removing those nodes which deliver maximum supply first can result in a nationwide low power situation. As a result, certain regions will be out of power, or government may ration the remaining capacity on the national level.

Demand Removing those nodes with the highest power demand first can result in local black-outs that affect areas with strong power demands, such as densely populated urban zones or industrial facilities.

Import Removing those nodes which provide import supplies first can also result in a nationwide low power situation. Whereas import nodes can be attacked both from within and beyond the national border, any national government can only protect nodes within the border. Hence, any country that must rely on foreign energy imports is particularly vulnerable if the attacker employs this strategy.

Export Removing those nodes which export power abroad first can result in power shortages or black-outs in neighboring countries. This effect also destabilizes the national grid, such that high demand for ancillary services that can compensate for the lack of demand is generated.

Topological An attacker striving to exploit the topological structure of the grid would minimize the number of attacked nodes while targeting those with the highest topological relevance for network performance. The relevance of each node can be measured by its *betweenness centrality* [7], which measures how often each node appears on a shortest path between any two nodes. Since there can be several shortest paths between two nodes s and t, the betweenness centrality of node v is:

$$C_B(v) = \sum_{s \neq t \neq v \in N} \frac{n_{st}(v)}{N_{st}} \tag{11}$$

where N_{st} is the total number of shortest paths from node s to node t and $n_{st}(v)$ is the number of those paths that pass through v. A high betweenness centrality value $C_B(v)$ implies that many shortest paths pass through the node v and therefore the node must have a topologically central position within the graph.

Whenever such central nodes are removed, the network loses multiple edges and the graph splits into subgraphs. As a result, regional power networks are disconnected from each other, implying the breakdown of the national transmission grid.

Terrorism An (N-1) analysis can be conducted for each node of a graph, i.e. a node is removed from the initial graph, the reduced graph is analyzed using the UD measure and afterwards the removed node is reintegrated before the next node is removed. As a result, discrete UDs are known, such that an attacker can target those with the highest UDs. This attack strategy can be deployed with little effort while it substantially reduces covered power demand. Contemporary computing equipment can calculate the respective UD values in a very short time. In our subsequent illustration, calculation for a power grid with 134 nodes and 394 edges was done in 38 s.[4]

Optimized Terrorism The above iterative approach can be extended in order to identify maximum UD when multiple nodes are removed. While computing time grows exponentially with network complexity (e.g. removing three nodes in a network with N nodes results in $N \cdot (N-1) \cdot (N-2)$ simulation runs), the power grid can be systematically analyzed in finite time to find those nodes whose joint removal implies maximum damage for the power grid.

3.2 Edge Removal

Transmission Lines with Maximum Power Flow Transmission lines can be easily attacked because they run outdoors and bridge long geographical distances. Whenever an edge is about to reach its maximum transmission capacity—as indi-

[4]Server infrastructure: 4x Intel Xeon Gold 6150 18C 165W 2.7 GHz CPU with 1.0 TB RAM.

cated by small RFC—and cannot be substituted by redundant edges, it constitutes a high-value target. The removal of such edges creates uncovered demand.

Transmission Lines with Maximum UD Similar to the node removal strategies *terrorism* and *optimized terrorism*, UDs can be calculated for both discrete and joint removal of edges. Hence, edges with the highest UDs are identified as attack targets. This identification also reveals edges critical for grid topology, e.g. those which import or export power, bridge subgraphs, or link significant supply and demand.

4 Simulation

The Swiss maximum voltage power grid transmits power by 380 kV and 220 kV transmission lines [16]. We modeled this grid as a directed graph with 159 nodes[5] and 394 bidirectional edges. Topological data for this network was obtained from a publicly available map created by the European Network of Transmission System Operators for Electricity [8]. Geocoordinates for each node were obtained from public Swisstopo data [5]. We imported these into Matlab R2017b and plotted them onto a map provided by d-maps.com [17]. Since we focus on the Swiss power grid, we modeled only nodes and edges within the national border, with the exception of 19 neighboring nodes in Germany, Austria, Italy and France that transmit imports and exports of power. Figure 2 superimposes our model onto a map of Switzerland.

4.1 Capacity Model

After this topological structure was defined, we attributed it with actual transmission flows and capacities. During this process, we made three assumptions to simplify the analysis.

First, we did not consider seasonal demand variation (e.g., higher power demand during the winter months due to heating). We can therefore work with annual demand and supply figures which are publicly available. Second, we did not consider dynamic electrophysical effects. Third, we assumed that any node connected to both a 380 kV and a 220 kV transmission line can transform any quantity of power between these voltage levels in either direction.

Energy Demand Energy demand was calculated for each node based on the overall energy consumption in Switzerland in 2013, i.e. a total consumption of 59,323 GWh [14]. We spread this national consumption over the cantons (federal states) of Switzerland by their respective population. We then further subdivided

[5]These 159 nodes comprise 134 physical supply and demand nodes as well as 25 auxiliary nodes we introduced to capture multiple connections.

Fig. 2 The Swiss maximum voltage power grid as a graph with 159 nodes and 394 edges (simplified representation)

these cantonal consumptions according to the nodes present in each canton. The demands from cantons where no node is present were distributed to the demands of the surrounding cantons.

We excluded the ten most populous cities from this subdivision and added them separately to the closest node instead.[6] Hence, all nodes within a canton have the same energy demand but for those nodes closest to the most populous cities. These latter nodes are modeled with a higher demand to reflect the larger power demand of urban areas.

Energy Supply Energy supply by nuclear power stations and run-of-river and storage power plants is assumed to be constant and hence the minimal and maximal values are equal ($supply_i^{min} = supply_i^{max}$). For the supply of pump storage, the calculated values have been used as the maximal values $supply_i^{max}$ and the minimal values have been set to $supply_i^{min} = 0\,\text{GWh}$.

Import Supplies and Export Demands Import supplies and export demands were calculated based on the annual supply and demand of each neighboring country [17] and divided by the number of nodes in the respective country.

Transmission Line Capacities Transmission line capacities x_{ij}^{max} were calculated based on the formula for the maximum (thermal) transmission capacity [2, p. 27]: $Power = \sqrt{3} \cdot U \cdot 4 \cdot I_{max}$ where U is the voltage level and I_{max} is the maximum allowed current of a single conductor while the factor 4 in the formula relates to the number of conductors in the line, i.e. a conductor bundle of four conductors. We assumed the bundle was of type 243-AL1/39- ST1A since this material is used most frequently in maximum voltage transmission grids. The corresponding maximum current is $I_{max} = 645\,\text{A}$ [2, p. 20]. Each of the 380 kV lines have been modeled with four conductors while each of the 220 kV lines have been modeled with two conductors [9, p. 92]. The transmission capacity was calculated on an annual basis ($Power \cdot 365\,\text{days} \cdot 24\,\text{h/day} \cdot 3600\,\text{s/h}$) and transformed from Joule to GWh (division by 3.6E+12). This procedure gave the capacities shown in Table 1.

4.2 Calculation

We created two Excel worksheets, one with all topological node data, demands and supplies, and one with all transmission capacities of all edges. These two Excel worksheets were imported into Matlab R2017b using the Spreadsheet Import Tool to generate a database container (*.mat) file.

[6] For example, two nodes supply power to the canton of Geneva. This canton has 280,400 inhabitants, of which 189,033 dwell in the city of Geneva. One of the two nodes is closer to the city, hence, in our model this node supplies power to 329,233 inhabitants (280,400/2 + 189,033). The second node supplies power to the remaining 140,200 (280,400/2) inhabitants.

Table 1 Transmission line capacities

Line types	First line [kV]	Second line [kV]	Third line [kV]	Transmission capacity [GWh]
Line type 1a	220	None	None	4310
Line type 1b	380	None	None	14,900
Line type 2a	220	220	None	8620
Line type 2b	380	220	None	19,210
Line type 2c	380	380	None	29,800
Line type 3a	380	220	220	23,520
Line type 3b	380	380	220	34,110
Line type 3c	380	380	380	44,700

We then used the `graph` function to generate a Matlab graph structure. We used the `conncomp` function to analyze if a graph was split into subgraphs upon a particular removal strategy. For all graphs and subgraphs, we used the function `linprog` to solve the optimization problem as stated in (5) to (8).

Whenever a node or edge removal strategy involved multiple removals, this procedure was used iteratively. For the topological strategy, betweenness centrality was calculated by Matlab's `centrality` function. Finally, uncovered demand was calculated and plotted as a function of node or edge removal.

4.3 Results

4.3.1 Node Removal

We iteratively removed each node of the graph and analyzed whether the resulting graph had split into subgraphs. We then solved the linear program as stated in (5) to (8). If the resulting grid could not cover the full demand, this demand was reduced as described in step 4 of Sect. 2.2, i.e. by setting the demand of the node with the smallest demand to zero (load shedding). For security reasons, the following results are presented by node and edge coding id's only, and geocoordinates are omitted.

For each removed node, uncovered demand was calculated according to (9) as a percentage of total demand. Figure 3 presents the results of this (N-1) analysis. The grid exhibits significant scale free properties [9], i.e. very few nodes are of constitutive importance to the grid, and their removal may cause the network to collapse. In our calculation, the removal of 93 nodes (i.e., 69% of all nodes in the networks) caused UDs of less than 1%, whereas these increased to between 8.8% and 11.1% when one of the demand nodes D6, D9, D15, D17 or D18 was removed.

We then simulated each node removal strategy as outlined in Sect. 3.1. Each strategy was calculated in two variants in which three and five nodes were removed, respectively. After these multiple removals the graph was inspected for splitting into

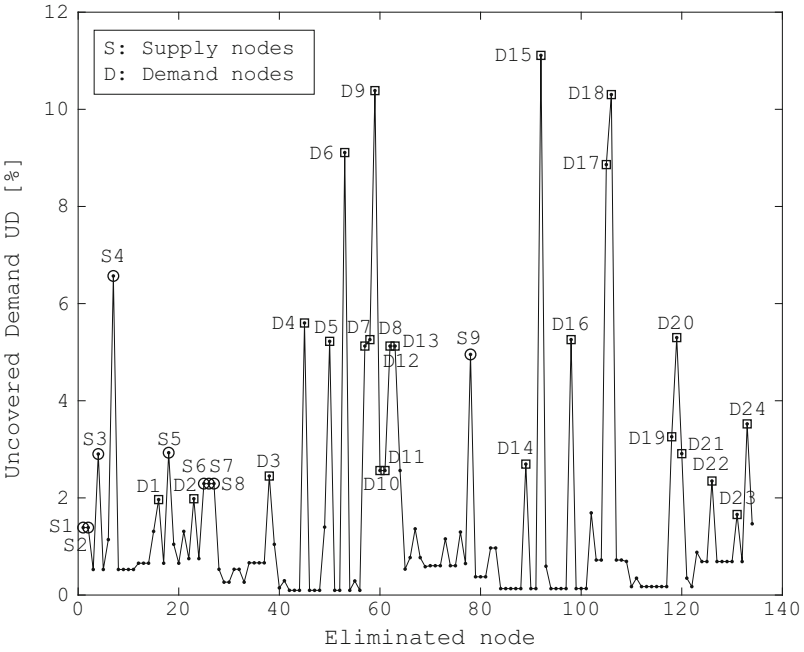

Fig. 3 Uncovered demand (UD) as a function of discrete node removal. We labeled nodes whose removal caused the largest uncovered demands by circles (supply nodes) and squares (demand nodes)

Table 2 Uncovered demands as a function of multiple node removal

Attack strategy	UD_{3nodes}	UD_{5nodes}
Supply	20.2%	25.1%
Demand	7.9%	13.3%
Import	15.5%	25.8%
Export	12.6%	20.7%
Topological	8.4%	20.3%
Terrorism	20.0%	26.1%

subgraphs; then, the optimization problem was solved. Table 2 presents the resulting uncovered demands by strategy and variation.

Removing nodes according to the *Supply*, *Import* and *Terrorism* attack strategies had the strongest negative effect on the Swiss power grid. By the removal of only five nodes (i.e., 3.7% of the grid), an uncovered demand of at least 25.1% results. By contrast, the removal of nodes with the highest demands according to the demand strategy resulted in the smallest UD values of all variants (7.9% and 13.3%, respectively).

Finally, the removal of those five nodes with maximum topological impact split the graph into six subgraphs and implied a loss of 62 edges, i.e. 15.7% of all edges.

When only three of these nodes were removed, the graph did not split, but still 32 edges were lost.

4.3.2 Edge Removal

Consistent with our explanations in Sect. 3.2, we ran two simulations for edge removal analysis. First, we simulated the discrete removal of edges with maximum transmission capacity and calculated the resulting UDs. Second, we performed an (E-1) analysis on the grid by discretely removing edges one by one, identifying those whose removal caused the highest UDs. Once these edges were known, they were eliminated from the graph to simulate the consequences for the grid.

The 394 bidirectional edges in our model correspond to 197 physical transmission lines in the grid. Figure 4 shows the absolute energy flows transmitted by these lines. It also gives the residual flow capacity (RFC) for each edge. With an average RFC of 86.6%, the grid seems to have much spare capacity by which power could be rerouted, and hence it appears relatively robust against random malfunction or loss of transmission lines. However, this picture changes when more deliberate attack patterns are considered.

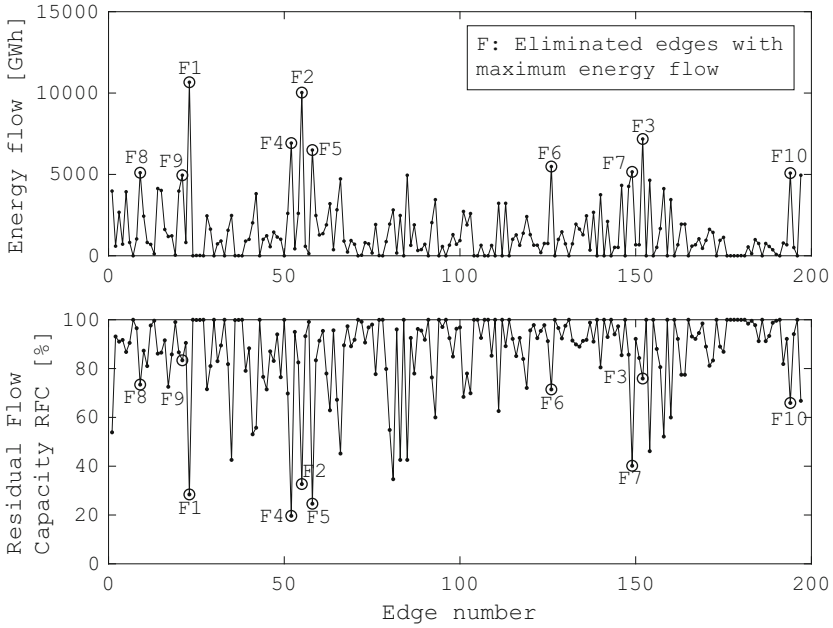

Fig. 4 The upper plot shows the energy flows of all the 197 transmission lines. The lower plot shows for each edge the Residual Flow Capacity as defined in Eq. (10) that relates the maximum flow values of the upper plot to the maximum flow capacities of each edge. The ten edges with the highest energy flow have been marked with a circle and labeled by F in both plots

Table 3 Uncovered demands (UD) after removing three, five or ten edges

Attack strategy	UD_{3nodes}	UD_{5nodes}	$UD_{10nodes}$
Maximum power flow	10.4%	15.6%	20.8%
Maximum UD	15.6%	20.6%	34.1%

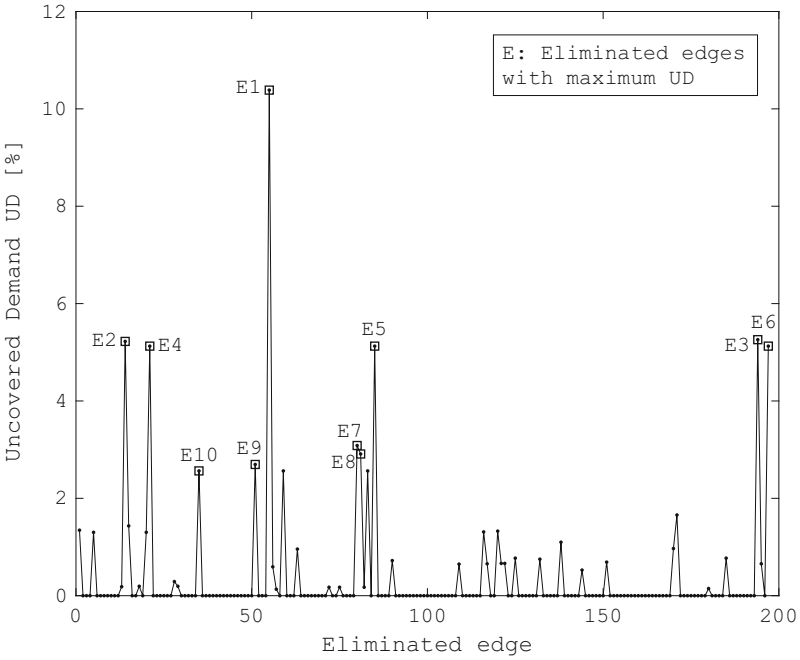

Fig. 5 Uncovered demand (UD) as a function of edge removal. Edges whose removal causes the highest UDs are marked with a square and labeled by E

Table 3 gives UDs when three or more edges are removed. For example, the removal of edges F1 to F10 which transmit the largest power flows in the network results in a UD of 20.8%.

Figure 5 presents the results of an (E-1) analysis for all 197 edges. The results corroborate the finding of the node removal analysis, i.e. the Swiss maximum voltage grid has significant scale free properties.

By contrast, some edges are of constitutive importance for the grid. The removal of any of the edges E2, E3, E4, E5 or E6 generates UDs of more than 5.1%, and the removal of E1 alone generates a UD of 10.4%. When those ten edges whose discrete elimination causes the highest respective UD values are removed in conjunction, a UD of 34.1% results (Table 3). This implies the grid is highly vulnerable, since the grid's transmission capacity can be reduced by a third by targeting only 5% of all edges.

5 Discussion

This simulation has modeled the Swiss maximum voltage transmission network as a graph and used linear programming techniques to analyze the resilience of this network. At a first glance, this grid appears relatively robust to cases of random and isolated component failure, since such events only result in minor performance loss. We find that the discrete removal of 69% of all nodes and 93% of all edges has a performance impact of close to nil, implying that power production can be managed and rerouted flexibly in the case of a probabilistic event.

However, this picture changes when deliberate attacks are considered. While the Swiss maximum voltage power grid is relatively robust against random failure of single components, deliberate attacks that follow a particular strategy can inflict significant damage to the grid. Both the node and the edge removal analyses demonstrate that significant uncovered demand is caused as a result of the removal of few yet topologically important elements. In particular, the node removal analysis suggests that removing supply (power-producing) elements from the network causes significantly more damage than removing demand (power-consuming) elements, such as urban areas. This implies the network we studied could adapt relatively well to demand failure by reducing supply, but would struggle to maintain performance upon supply failure.

Our modeling approach has made a number of simplifying assumptions that future research could relax. For example, we assumed that any node connected to both 220 kV and 380 kV lines has unlimited transformation capacity between these voltage levels. The resulting estimates for uncovered demand can thus be interpreted as best case scenarios, since the introduction of a restriction factor that limits transmission capacity puts further stress on the grid in the case of attacks. Future research may therefore expand our approach by putting more emphasis on the electro-physical and electro-dynamic restrictions of a power grid.

Prior literature has focused on the topological analysis of power grids, with the goal of identifying bottlenecks among both power supply and transmission elements [9, 12]. However, our results caution the reader to rely on topological analysis alone since this focus is unlikely to provide a full picture of the damage that deliberate attacks could cause. Our node removal analysis showed that, while the topological attack strategy causes an uncovered demand of 20.3% by removing five nodes with high betweenness centrality, the supply, import, and terrorism strategies inflict even greater damage. Hence, even a topological redesign of the network that emphasizes greater redundancy would not prevent such attacks. In this respect, the edge removal analysis shows that more edges than nodes must be removed to inflict similar damage, but since edges can be attacked more easily than nodes, targeted terrorism against transmission lines remains a feasible attack strategy.

The feasibility of deliberate attacks therefore confronts power grid operators with significant architectural challenges, and building resilient networks that can withstand deliberate attack patterns is at the core of this challenge. In all the analyzed attack patterns, the attacker has an advantage since the attacker chooses

the strategy, the time and the intensity of the attack. The operators can neither foresee nor prevent such attacks with certainty. At the same time, an all-hazard approach that intends to protect the complete grid against any potential attack implies prohibitively high cost and hence is economically not viable for a grid operator even if such protective structures can be built. Hence, a more cost-effective approach is to increase the resilience of the network by reducing the damage any attack can infer onto the grid. As such resilience renders attacks futile, the attacker is also "educated" that any attack will be of little consequence. In this respect, three measures should be considered which, by themselves or in conjunction, should increase the resilience of any power grid.

First, operators can control temporary disequilibria between power supply and demand by applying ancillary services [2]. However, today's services were not designed to withstand deliberate attacks, and hence large-scale safety capacity should be created that can bridge supply gaps at any time and for longer periods of time. Our simulation suggests that deliberate attacks can cause uncovered demand that exceeds 20% of supply. In today's grids, such significant loss would immediately result in cascading load shedding, such that certain regions will be without power or power has to be rationed. Future safety capacity must be built to a scale that can cover such losses until the grid can be stabilized. Second, as existing power grid nodes and edges are replaced at the end of their technological lifecycle, future grid construction should strive to both reduce the betweenness centrality of nodes wherever possible and to add redundant edges with large residual flow capacity that can reroute power. This redundancy can be further strengthened by robust construction methods, e.g. by tunneling transmission lines through subsurface infrastructure instead of letting them run in open air. Of course, this robust construction comes at a price since air can no longer be used as an isolator, implying higher construction cost due to the adverse thermodynamic properties of subsurface transmission lines. Third, by definition the strategic importance of any transmission grid declines as the supply of power can be decentralized. Private and industrial consumers of energy should therefore emphasize the construction of autonomous and regional elements that can reliably supply power on a regional or local level even if the national grid should be compromised.

References

1. Albert, R., Albert, I., Nakarado, G.L.: Structural vulnerability of the north american power grid. Phys. Rev. E **69**(2), 025,103 (2004)
2. Ausbau elektrischer Netze mit Kabel oder Freileitung unter besonderer Berücksichtigung der Einspeisung Erneuerbarer Energien. http://www.izes.de/
3. Bernstein, A., Bienstock, D., Hay, D., Uzunoglu, M., Zussman, G.: Power grid vulnerability to geographically correlated failures – analysis and control implications. In: INFOCOM, 2014 Proceedings IEEE, pp. 2634–2642. IEEE, Piscataway (2014)
4. Bompard, E., Napoli, R., Xue, F.: Analysis of structural vulnerabilities in power transmission grids. Int. J. Crit. Infrastruct. Prot. **2**(1), 5–12 (2009)

5. Bundesamt für Landestopografie swisstopo. http://www.swisstopo.admin.ch
6. Crucitti, P., Latora, V., Marchiori, M.: Model for cascading failures in complex networks. Phys. Rev. E **69**(4), 045,104 (2004)
7. Cuadra, L., Salcedo-Sanz, S., Del Ser, J., Jiménez-Fernández, S., Geem, Z.W.: A critical review of robustness in power grids using complex networks concepts. Energies **8**(9), 9211–9265 (2015)
8. European Network of Transmission System Operators, ENTSO-E. https://www.entsoe.eu
9. Fischer, R., Kießling, F.: Freileitungen: Planung, Berechnung, Ausführung. Springer, Berlin (2013)
10. Mei, S., Zhang, X., Cao, M.: Power grid complexity. Springer Science & Business Media, New York (2011)
11. Pagani, G.A., Aiello, M.: The power grid as a complex network: a survey. Physica A Stat. Mech. Appl. **392**(11), 2688–2700 (2013)
12. Pahwa, S., Scoglio, C., Scala, A.: Abruptness of cascade failures in power grids. Sci. Rep. **4**, 3694 (2014)
13. Sachtjen, M., Carreras, B., Lynch, V.: Disturbances in a power transmission system. Phys. Rev. E **61**(5), 4877 (2000)
14. Schweizerische Gesamtenergiestatistik 2013, Swiss Federal Office of Energy. http://www.bfe.admin.ch/
15. Solé, R.V., Rosas-Casals, M., Corominas-Murtra, B., Valverde, S.: Robustness of the European power grids under intentional attack. Phys. Rev. E **77**(2), 026,102 (2008)
16. Stromübertragungsnetz zuständige Landesgesellschaft, Swissgrid AG. https://www.swissgrid.ch
17. Swiss national map from d-maps.com. http://www.d-maps.com/carte.php?num_car=24779&lang=de
18. Zhang, G., Li, Z., Zhang, B., Halang, W.A.: Understanding the cascading failures in Indian power grids with complex networks theory. Physica A Stat. Mech. Appl. **392**(15), 3273–3280 (2013)